FI SEVIER

Contents lists available at ScienceDirect

International Journal of Thermal Sciences

journal homepage: www.elsevier.com/locate/ijts



Evaluating the influence of thermal dispersion on temperature plumes from geothermal systems using analytical solutions

Nelson Molina-Giraldo ^{a,*}, Peter Bayer ^b, Philipp Blum ^c

- ^a University of Tübingen, Center for Applied Geoscience (ZAG), Sigwartstraße 10, 72076 Tübingen, Germany
- ^b ETH Zürich, Engineering Geology, Sonneggstrasse 5, 8092 Zurich, Switzerland
- ^c Karlsruhe Institute of Technology (KIT), Institute for Applied Geosciences (AGW), Kaiserstraße 12, 76131 Karlsruhe, Germany

ARTICLE INFO

Article history:
Received 12 May 2010
Received in revised form
7 December 2010
Accepted 7 February 2011
Available online 16 March 2011

Keywords:
Thermal dispersion
Plume length
Borehole heat exchanger
Aquifer
Analytical solution
Geothermal energy

ABSTRACT

An analytical study is carried out to examine the effect of thermal dispersion on the simulation of temperature plumes in aquifers that evolve from vertical ground source heat pump (GSHP) systems. Analytical solutions for the simulation of heat transport in aquifers often ignore thermal dispersion. In this study an existing two-dimensional analytical approach for transient conditions is used. Moreover, an equation to calculate the length of the temperature plume for steady state conditions is developed. To study the interplay between thermal dispersion and hydraulic conductivity, Darcy velocities are varied from 10^{-8} m/s to 10^{-5} m/s and thermal dispersivities are varied based on two assumptions: 1) thermal dispersion is assumed to be only dependent on the Darcy velocity and 2) thermal dispersion is assumed to be scale-dependent. The results are discussed with respect to their implications for typical legal regulations and operation of such GSHP systems. In general, the effect of thermal dispersion on the temperature plume around the borehole heat exchanger (BHE) is minor when thermal dispersion is assumed to be depending solely on the magnitude of groundwater flow (e.g., in a homogeneous aquifer). On the other hand, based on a field scale of 10 m and assuming thermal dispersion to be scale-dependent, thermal dispersion can be neglected only for conditions typical for fine sands, clays, and silts with $q < 10^{-8}$ m/s. For aquifers where medium sands and gravels (with Darcy velocities $q > 10^{-8}$ m/s) dominate, thermal dispersion has a larger effect on the temperature plume distribution around the borehole heat exchanger.

© 2011 Elsevier Masson SAS. All rights reserved.

1. Introduction

The use of shallow geothermal energy is continuously increasing [1] and in particular the application of vertical ground source heat pump (GSHP) systems [2]. This technology relies on a simple concept: One or more vertical pipes are installed down to depths of around 50 m—150 m [3]. The pipes act as borehole heat exchangers (BHEs) that are connected to an aboveground heat pump. Heat exchange is accomplished by circulation of a heat carrier fluid within this closed system. The energy from underground is mostly used for space heating and warm water supply. Alternatively, during warm seasons or when superfluous heat is available, energy can also be injected for storage or to support airconditioning systems. Geothermal energy is counted among the renewable resources. It offers environmental benefits, since

considerable amounts of fossil fuel can be saved and thus additional CO_2 emissions can be avoided or even reduced [4,5].

The use of GSHP systems yields temperature plumes in the subsurface, which can extend to a significant size and prevail for a long time depending on the hydrogeological conditions and mode of the system, heating or cooling [6–8]. The length of the temperature plume is defined as the distance downgradient from the injection/extraction point to the isotherm contour of interest. Temperature plumes that adversely affect adjacent and neighboring geothermal systems have to be avoided. Thus, they have to be well predicted and controlled to guarantee long-term sustainable use. In some countries, minimum distances between two BHEs and maximum temperature changes allowed in the underground are required. For instance, in the German state of Baden-Württemberg, a distance of 10 m between individual BHEs is suggested by the regulators [7,9]. In Switzerland, a distance of 4 m–8 m is typically recommended between individual BHEs.

Numerical models are widely applied to simulate heat transport in aquifers under the influence of GSHP systems [10–12]. Chiasson

^{*} Corresponding author. Tel.: +49 7071 2973172; fax: +49 7071 5059. E-mail address: nelson.molina-giraldo@uni-tuebingen.de (N. Molina-Giraldo).

Nomenclature		Z	argument of the Bessel function	
С	specific heat capacity (J/kg/K)	Greek	symbols	
d	mean particle diameter (m)	α	thermal dispersivity (m)	
K	hydraulic conductivity (m/s)	λ_{x}	effective thermal conductivity in the longitudinal	
K_0	modified Bessel function of second kind and order zero		direction (W/m/K)	
L	field scale (m)	λ_{v}	effective thermal conductivity in the transverse	
L_p	plume length (m)	,	direction (W/m/K)	
n	total porosity	$\lambda_{\mathbf{o}}$	bulk thermal conductivity of porous medium (W/m/K)	
Pe	Peclet number	$\lambda_{\mathbf{d}}$	thermal dispersion coefficient (W/m/K)	
q	Darcy velocity (m/s)	ρ	density (kg/m³)	
R_T	retardation factor	φ	integration parameter	
q_L	heat flow rate per unit length of the borehole (W/m)			
t	time (s)	Subscr	Subscripts	
T	average temperature of the porous medium (°C)	S	aquifer material (solids)	
ΔT	temperature change (°C)	w	water	
S	volumetric heat source (W/m³)	<i>x</i> , <i>y</i>	longitudinal and transverse direction	
<i>x</i> , <i>y</i>	space coordinates (m)		-	
$ \begin{array}{c c} q_L \\ t \\ T \\ \Delta T \\ s \end{array} $	heat flow rate per unit length of the borehole (W/m) time (s) average temperature of the porous medium (°C) temperature change (°C) volumetric heat source (W/m³)	Subscr s w	ripts aquifer material (solids) water	

et al. [10] and Fan et al. [11] evaluated the effects of groundwater flow on the heat transfer into the BHE of GSHP systems. They concluded that groundwater flow enhances heat transfer between the BHE and the aquifer. Hidalgo et al. [12] carried out steady state numerical simulations for temperature plumes of BHEs. The principal aim was to find out the influence of hydraulic conductivity heterogeneity on heat transport and thus evaluate the effect of thermal dispersion. Such numerical models are in particular suitable for complex configurations and boundary conditions.

Analytical models are fast and straightforward means to calculate the expected extension of temperature plume, as long as simple configurations are studied and homogeneous aquifers can be assumed. Some analytical approaches to simulate heat transport in the subsurface presume conduction-dominated systems [13]. Heat is transported by thermal diffusion along a temperature gradient and thus the role of groundwater flow (advection) is not taken into account. These types of analytical solutions are based on the line-source theory and are widely used for the evaluation of geothermal applications such as BHE and thermal response tests [14].

However, if groundwater velocity is present, advective transport has to be considered. Then heat is transported by the moving water, and differential advection occurs due to the different flow pathways that are possible in porous media. This process is called thermal dispersion, and is generated by microscale mixing of the pore-scale interstitial water [15,16] as well as by differential transport in macroscale geological heterogeneities [12,17—19]. Usually, the dominant process is thermal diffusion [15].

Analytical approaches are available that model the effect of groundwater flow for an infinite line-source [13,20,21]. However, these do not consider thermal dispersion. Even if thermal diffusion is dominant, the error introduced from this simplification is rarely discussed. Depending on the nature of the aquifer, mechanical mixing of heat due to differential convection at the microscopic scale and heterogeneities of the conductivity field can affect the spreading of the heat plume in the subsurface [12,18,22]. Therefore, an evaluation of the importance of considering thermal dispersion in the regulation and monitoring of GSHP systems is required.

In this study an existing two-dimensional (2D) analytical approach for transient conditions which considers thermal dispersion is used. Metzger et al. [23] developed this analytical solution to determine thermal dispersion coefficients for a packed bed of glass spheres. This analytical solution, however, has not been applied yet for GSHP systems. In the present study, the latter transient solution is reduced to steady state conditions and an equation to calculate the length of the temperature plume is

developed. The principal aim is to analytically characterize the role of thermal dispersion on the simulation of temperature plumes, which develop from GSHP systems in typical natural aquifers. The results are discussed with respect to their implications for the operation of GSHP systems under typical legal regulations such as on the suggested minimum distance between single borehole heat exchangers (BHEs) and neighboring installations.

2. Governing equations

2.1. Heat transport in the subsurface

Heat transport in porous media is accomplished mainly by conduction through the fluid and solid phase and advection through the moving water. Therefore, it is characterized by the heat advection/dispersion equation, which can be expressed in a 2D form (x-y plane) as follows [17]:

$$\rho c \frac{\partial T}{\partial t} + q \rho_w c_w \frac{\partial T}{\partial x} - \lambda_x \frac{\partial^2 T}{\partial x^2} - \lambda_y \frac{\partial^2 T}{\partial y^2} - s = 0$$
 (1)

where T denotes the average temperature of the porous medium in which local thermal equilibrium is assumed [24], q is the uniform Darcy velocity in the x-direction, s is a volumetric heat source, and ρc is the volumetric heat capacity of the bulk porous medium. The latter can be computed as the weighted arithmetic mean of the solids of the aquifer ($\rho_s c_s$) and water ($\rho_w c_w$) [17]:

$$\rho c = n\rho_w c_w + (1 - n)\rho_s c_s \tag{2}$$

The effective longitudinal and transverse thermal conductivities, λ_x and λ_y are defined by two components: the bulk thermal conductivity of the porous medium (λ_0) in the absence of groundwater flow and dispersion quantified by the thermal dispersion coefficient (λ_d):

$$\lambda_{X} = \lambda_{0} + \lambda_{d,X} \tag{3}$$

$$\lambda_{\mathbf{y}} = \lambda_{\mathbf{0}} + \lambda_{\mathbf{d}, \mathbf{y}} \tag{4}$$

2.2. Thermal dispersion

Thermal diffusion and convection are the two main processes involved in the thermal dispersion coefficients given by equations (3) and (4). Heat transported by temperature gradients within the

fluid/solid phase is represented by λ_0 . Upon convection the heat is also transported by the moving water itself and differential convection occurs due to the different flow pathways that are possible in porous media. These variations in magnitude and direction of the velocity field at the pore-scale create the so-called thermal dispersion (λ_d) [15,16]. In addition, differential heat transport due to the heterogeneity of the permeability field at macroscopic scales also contributes to thermal dispersion [12,15,17–19]. Ferguson [18] and Hidalgo et al. [12], for instance, emphasize that thermal dispersion is linked to the spatial variability of the hydraulic conductivity field which causes considerable uncertainty about the spreading of the heat plumes in the subsurface.

Traditionally, thermal dispersion has been neglected in heat transport simulation problems because of the dominance of thermal diffusion ($\lambda_0/\rho c$) [15,25,26]. This is reflected by remarkable thermal diffusion coefficients, which are commonly much higher than those coefficients describing solute diffusion [15,26]. Typical values of solute diffusion coefficients for small molecules are in the order of 10^{-9} m²/s, whereas values for thermal diffusion coefficient are in the order of 10^{-7} m²/s [27]. One further argument for such simplification is the higher computational effort for numerical modeling of dispersive heat transport. In addition, acquisition of reliable thermal dispersion values would imply additional field measurements and/or calibration procedures.

Thermal dispersion coefficient is usually assumed to be dependent on the fluid velocity and particle size of the porous media [16,23,28–31]. Metzger et al. [23], for instance, estimated thermal dispersion coefficients under different fluid velocities scenarios for a packed bed (40 cm \times 10 cm) of glass spheres (d=2 mm). Based on their experimental results, they proposed the following correlations:

$$\frac{\lambda_{x}}{\lambda_{w}} = \frac{\lambda_{o}}{\lambda_{w}} + APe^{m_{1}} \tag{5a}$$

$$\frac{\lambda_y}{\lambda_{w}} = \frac{\lambda_o}{\lambda_{w}} + APe^{m_1} \tag{5b}$$

where A=0.073 and $m_1=1.59$ for the longitudinal dispersion correlation (λ_x/λ_w) and A=0.03 (lower limit) or 0.05 (upper limit) and $m_1=1.00$ for the transverse dispersion correlation (λ_y/λ_w) . The Peclet number (Pe) which relates the energy transported by advection to the energy transported by conduction is expressed in equation (5) as:

$$Pe = \frac{\rho_w c_w q d}{\lambda_w} \tag{6}$$

where d denotes the mean particle diameter.

Although these kinds of correlations are well accepted in engineering applications, they are uncommon in geothermal modeling. This is mainly due to the fact that they are based on controlled lab experiments with homogenous porous media and the uncertainty introduced by macroscale heterogeneities of hydraulic conductivity is not accounted for. Sauty et al. [32] and de Marsily [17] proposed a thermal dispersion coefficient, similar to solute transport [15], where the thermal dispersion term is related to the heterogeneity of the velocity field and is a linear function of this velocity. The following expressions are used by modelers to represent what they do not know about the exact structure of the aquifer and its heterogeneity [19,33–36]:

$$\lambda_{X} = \lambda_{o} + \alpha_{X} \rho_{w} c_{w} q \tag{7}$$

$$\lambda_{V} = \lambda_{o} + \alpha_{V} \rho_{w} c_{w} q \tag{8}$$

The degree of the thermal dispersion coefficient depends on the direction relative to flow. In two dimensions, this is reflected by two dispersivity terms, a longitudinal (α_x) and a transverse (α_y). The relationship of $\alpha_y = 0.1\alpha_x$ is commonly assumed for solute transport [27,37], and also for thermal transport [e.g., 33,34,36,38]. However, this relationship might vary depending on the heterogeneity structure of the aquifer [39] and the Peclet number [15,22,27].

In the area of solute transport, numerous studies on theoretical and experimental investigations were carried out on dispersion in aquifers [37,39–42]. They indicate that the solute longitudinal dispersivities are scale-dependent (i.e., dispersion depends on the distance traveled by the solute particle). Hence, in the literature some equations relating the field scale and the solute longitudinal dispersivity can be found. In general, they are expressed by the following empirical relationship [40–42]:

$$\alpha_{x} = b(L)^{m_2} \tag{9}$$

where L represents the field scale, and b and m_2 characteristic coefficients of the geological medium. Results from different empirical equations are plotted in Fig. 1. Obviously a large range and uncertainty depending on the applied relationship exists. For instance, using a field scale of 10 m, the longitudinal dispersivity might be 0.5 m, 0.8 m or 2 m, depending entirely on the applied empirical relationship.

Measured and experimental thermal longitudinal dispersivity values reported in the literature [17,19,33,37,38,43—45] are shown in Fig. 1. Most of these values are located within the ranges given by the empirical relationships derived for solute transport. This also reflects that geological conditions can be highly variable with different representative values of thermal dispersivity.

Windqvist and Hyden [46], cited in Sauty et al. [19], carried out a comparison between heat and solute transport in a Swedish aquifer. The results indicated similar dispersivities for both processes. Sauty et al. [19] developed in-situ experimental investigations of hot water storage in a confined aquifer and determined values of thermal dispersivity indirectly by model calibration. They stated that the calculated value of thermal dispersivity was of the same order of magnitude as that obtained with a tracer test at the same site. de Marsily [17] presented a single field experiment with both solute and thermal tracer tests. He showed that the thermal and solute longitudinal dispersivities are similar and therefore can be used as equivalent parameters. Yuan et al. [47] carried out a theoretical study on thermal dispersion in porous media. They conclude that thermal dispersion varies over a wide range as a result of heterogeneities. Ferguson [18] and Hidalgo et al. [12]

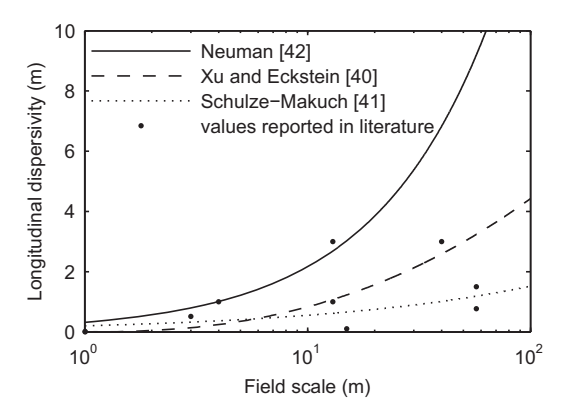


Fig. 1. Relationship between field scale and solute longitudinal dispersivity for different empirical relationships (solid and intermittent lines) [40,41,42]. Values of thermal longitudinal dispersivities reported in literature are shown as dots [17,19,33,37,38,43,44,45].

related thermal dispersion to the heterogeneity of the hydraulic conductivity field suggesting that thermal dispersion is somehow linked to the field scale. Under steady state conditions, transverse dispersivity is, for instance, related to the variance of the hydraulic conductivity $\sigma_{\text{ln}K}^2$ and the correlation length L_x of an anisotropic Gaussian semivariogram [12]:

$$\alpha_{V} = 0.02\sigma_{\ln K}^{2}L_{X} \tag{10}$$

For the conditions simulated by Hidalgo et al. [12], transverse dispersivities vary from 2 to 6 m for a model domain of $1000 \times 500 \times 500$ m (x, y, z direction).

Vandenbohede et al. [48] performed two push—pull tests injecting chloride and cold water into an aquifer. Contrary to Windqvist and Hyden [46] and de Marsily [17], Vandenbohede et al. [48] state that thermal and solute dispersivities do not appear to be comparable. Furthermore, they did not observe a scale-dependency for thermal dispersivity. They argue that this is mainly due to the fact that contrary to solute transport, heat is not only transported through the fluid phase, but also throughout the solid phase. Hence, it is less influenced by heterogeneity. Constantz et al. [44] offer a comparison of heat and solute tracer tests. They claim that thermal dispersivities are notably smaller than solute dispersivities.

In summary, it is still not clear whether the magnitude of the heat and solute dispersivities are the same and whether thermal dispersion is scale-dependent. However, one must have always in mind as explained by Vandenbohede et al. [48] and Bear [15] that thermal dispersion in heat transport might be not as significant as in solute transport due to the heat exchange between the fluid and the solid phase. This process is quantified by the retardation factor (R_T) which is given as the ratio between the volumetric heat capacities of the porous medium, ρc and water $n \rho_W c_W$:

$$R_T = \frac{\rho c}{n \rho_w c_W} \tag{11}$$

3. Analytical models

The solution of the partial differential equation (PDE) for heat transport in porous media (eq. (1)) for an infinite porous medium with an uniform initial temperature is given by [23]:

$$\Delta T(x, y, t) = \frac{q_L}{4\pi \sqrt{\lambda_x \lambda_y}} \exp\left[\frac{\rho_w c_w q x}{2\lambda_x}\right] \int_{0}^{\frac{(\rho_w c_w q y)^{-1}}{4\rho c_x^2}} \exp\left[-\phi - \left(\frac{x^2}{\lambda_x} + \frac{y^2}{\lambda_y}\right) \frac{(\rho_w c_w q)^2}{16\lambda_x \phi}\right] \frac{d\phi}{\phi}$$
(12)

This analytical solution applies for the response of a constant line-source with infinite length along the vertical (z) direction with a continuous heat flow rate per unit length of the borehole, q_L . This is a simplified but widely accepted approach to approximate the subsurface heat transport processes stimulated by GSHP operation [20,21,49]. Note that although the underground is assumed to be homogeneous in the analytical solution, "artificial" heterogeneity of the hydraulic conductivity field can be accounted for by a thermal dispersion term.

Metzger et al. [23] used this analytical solution (eq.(12)) to estimate thermal dispersion coefficients for a packed bed of glass spheres. For steady state conditions, equation (12) reduces to the following form:

$$\Delta T(x,y) = \frac{q_L}{2\pi\sqrt{\lambda_x\lambda_y}} \exp\left[\frac{\rho_w c_w qx}{2\lambda_x}\right] K_0 \left[\frac{\rho_w c_w q}{2}\sqrt{\frac{\lambda_y x^2 + \lambda_x y^2}{\lambda_x^2 \lambda_y}}\right]$$
(13)

in which K_0 is the modified Bessel function of the second kind of order zero.

If the thermal dispersion coefficients are set equal to zero $(\lambda_x = \lambda_y = \lambda_0)$, equations (12) and (13) reduce to the following analytical solutions given by Sutton et al. [20], Zubair and Chaudhry [50], and Diao et al. [21]:

$$\Delta T(x, y, t) = \frac{q_L}{4\pi\lambda_0} \exp\left[\frac{\rho_W c_W q x}{2\lambda_0}\right] \int_0^{\frac{(\rho_W c_W q)^2 t}{4\rho c \lambda_0}} \exp\left[-\phi - \frac{(\rho_W c_W q)^2 r^2}{16\lambda_0^2 \phi}\right] \frac{\mathrm{d}\phi}{\phi}$$
(14)

$$\Delta T(x,y) = \frac{q_L}{2\pi\lambda_0} \exp\left[\frac{\rho_W c_W qx}{2\lambda_0}\right] K_0 \left[\frac{\rho_W c_W qr}{2\lambda_0}\right]$$
(15)

where $r^2 = x^2 + y^2$. Sutton et al. [20] use this approach to calculate the ground resistance in BHEs. This ground resistance is an indirect measure of how much energy is resisted to flow to the ground. Zubair and Chaudhry [50] calculate temperature distributions in a homogeneous, isotropic, infinite medium for time-dependent energy extraction/injection. Diao et al. [21] employ the same equations to evaluate the effect of groundwater advection on GSHP systems.

The calculation of the plume length is complex due to the difficulty of expressing the plume length (L_p) as a function of a specific isotherm contour (ΔT) , i.e., $x = f(\Delta T)$. In the present study, an iterative interpolation method is used in MATLAB to compute the temperature plume length for a given ΔT under transient conditions.

For steady state conditions, however, an approximation can be made in order to calculate the length of the temperature plume. Equation (13) is first expressed in the following form:

$$\Delta T(L_p, 0) = \frac{q_L}{2\pi \sqrt{\lambda_x \lambda_y}} \exp\left[\frac{\rho_w c_w q L_p}{2\lambda_x}\right] K_0 \left[\frac{\rho_w c_w q L_p}{2\lambda_x}\right]$$
(16)

where L_p is the temperature plume length and ΔT is evaluated in the line of symmetry along the x-axis with y=0. The modified Bessel function of the second kind of order zero, $K_0(z)$, can be approximated by the following equation considering only the first two terms of the series expansion [13]:

$$z^{0.5} \exp(z) K_0[z] \approx \sqrt{\frac{\pi}{2}} \left(1 - \frac{1}{8z}\right)$$
 (17)

where z is the argument of the Bessel function. Substituting equation (17) into equation (16) gives the following quadratic equation:

$$\left(\frac{4\pi\rho_w c_w \lambda_y q \Delta T^2}{q_L^2}\right) L_p^2 - L_p + \frac{\lambda_x}{2\rho_w c_w q} = 0$$
 (18)

Finally, solving equation (18) for the temperature plume length (L_n) yields:

$$L_p = \left(\frac{q_L^2}{8\pi\rho_w c_w \lambda_y q \Delta T^2}\right) \left(1 \pm \sqrt{1 - \frac{8\pi\lambda_x \lambda_y \Delta T^2}{q_L^2}}\right)$$
(19)

Equation (19) can be used to calculate the length of a temperature plume (L_p) for a given isothermal contour (ΔT) under steady

state conditions. This approximation, however, is valid only for z >> 1. The relative error of the approximation is within 0.01 when z > 3 [51]. As an example, Fig. 2 shows a comparison of the approximation equation (eq. (19)) with the full solution (eq. (16)). For this specific case, the relative error is about 5% for a $\Delta T = -2$ K and for $\Delta T > -1.4$ K the relative error is lower than 1%.

4. Model set up

For the evaluation of the effect of thermal dispersion on temperature plumes, a 2D synthetic model is set up and solved analytically for transient and steady state conditions using equations (12)–(15). Table 1 provides typical hydraulic and thermal parameters for natural aquifer systems [17,52,53]. Hydraulic conductivities show a wide range over more than 8 orders of magnitude. In contrast, the variability of heat transport parameters is comparatively low.

Due to their low variability in nature, values of some thermal model parameters are fixed. Thermal conductivity and heat capacity of the bulk porous media are set to 2.5 W/m/K and $2.8\times 10^6\,\text{J/m}^3/\text{K}$, respectively. Accordingly, the thermal diffusivity is set to 9×10^{-7} m/s. These values are within the range of typical sand aquifers [17,52].

The influence of the other descriptive parameters is further scrutinized. Several groundwater flow scenarios are evaluated by varying hydraulic conductivity from 10^{-5} m/s to 10^{-2} m/s, which is within the range for typical sand and gravel aquifers (Table 1). Assuming a constant hydraulic gradient of 10^{-3} , the Darcy velocity (q) ranges from 10^{-8} m/s to 10^{-5} m/s. Darcy velocities lower than 10^{-8} m/s are not considered here, because thermal dispersion is expected to have only a minor effect under such conditions. Energy extraction is set to a typical value of -60 W/m, based on 2400 h (100 days) of operation during the year in a sand and gravel aquifer [54].

As reviewed above, there is some controversy regarding the scale dependence of thermal dispersivity and its similarity with solute dispersivity. Therefore, two assumptions are made: 1) thermal dispersion is assumed to be only dependent on the Darcy velocity (e.g., homogeneous aquifers). Hence, relationships proposed by Metzger et al. [23] are used and 2) thermal dispersion is assumed to be comparable to solute dispersion and scale-dependent.

In order to relate the thermal dispersion correlations given by equation (5) with the dispersivity terms (α_x , α_y), Equation (5) is

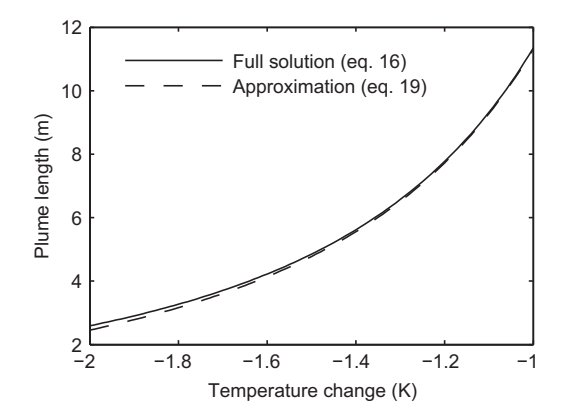


Fig. 2. Plume length for steady state conditions as a function of temperature change. Small discrepancies are observed between the predictions by the temperature plume length equation and by the full solution ($q = 2 \times 10^{-6}$ m/s, $\lambda_x = 7$ W/m/K, $\lambda_y = 3$ W/m/K, $\lambda_y = 3$ W/m/K, $\lambda_y = 6$ W/m, λ_y

Table 1

Hydraulic and thermal parameters for unconsolidated aquifer materials. Hydraulic conductivity, Darcy velocity, bulk thermal conductivity and volumetric heat capacity of porous medium are represented by K, q, λ_0 and ρc , respectively. Darcy velocity is calculated based on an hydraulic gradient of 10^{-3} . Values for λ_0 and ρc are for saturated aquifer materials.

Aquifer material	K [m/s]	q [m/s]	$\lambda_o[W/m/K]$	$ ho c imes 10^6 [J/m^3/K]$
Gravel	$10^{-4} - 10^{-2}$	$10^{-7} - 10^{-5}$	1.8	2.4
Coarse sand	10^{-3}	10^{-6}	1.7 - 5.0	2.2-2.9
Medium sand	10^{-4}	10^{-7}	1.7 - 5.0	2.2-2.9
Fine sand	$10^{-6} - 10^{-5}$	$10^{-9} - 10^{-8}$	1.7 - 5.0	2.2-2.9
Silt	10^{-7}	10^{-10}	0.9 - 2.3	1.6-3.4
Clay	$10^{-10} - 10^{-9}$	$10^{-13} - 10^{-12}$	1.2 - 1.5	2.3

compared with equations (7) and (8). This yields the following expression:

$$\alpha_{x,y} = A \left(\frac{\rho_w c_w q}{\lambda_w} \right)^{m_1 - 1} d^m \tag{20}$$

For the present study an upper limit of the Darcy velocity of 1×10^{-5} m/s is set, which represents a rather high velocity in natural porous aquifers. Assuming a particle diameter of 0.065 m, which is the maximum value for gravel, results in a longitudinal and transverse dispersivity of $\alpha_x=1\times 10^{-2}$ m (1 cm) and $\alpha_y=3.3\times 10^{-3}$ m (0.33 cm), respectively. These values are used for the first approach.

For the second approach, a field scale of 10 m distance downgradient from the point of energy extraction is chosen. This distance is based on the recommended minimum distance between two BHEs in the state of Baden-Württemberg, Germany [9]. For a field scale of 10 m, longitudinal dispersivities vary from 0.5 m to 2 m depending on the applied empirical relationship (Fig. 1). For the sake of simplicity, transverse dispersivities are set between 0.05 m and 0.2 m, assuming $\alpha_y = 0.1\alpha_x$ [33,34,36,38]. A summary of the resulting scenarios is presented in Table 2.

In order to assess the influence of thermal dispersion on the simulation of temperature plumes, simulations of temperature profiles along the centerline of the plume are carried out for a distance of 1 m–10 m downgradient from the source for steady state and transient conditions. The simulations are run for the range of Darcy velocities and thermal dispersivities as given above. An example of a temperature profile for steady state conditions is shown in Fig. 3.

Comparison of the results is based on the computed root mean square error (RMSE) which quantifies the residual error of the temperature profiles between the outputs with and without thermal dispersion as follows:

$$RMSE = \sqrt{\frac{\sum_{i=1}^{n} \left(\Delta T_{o(i)} - \Delta T_{(i)}\right)^{2}}{n}}$$
 (21)

in which $\Delta T_{(i)}$ corresponds to the results from the analytical solution considering thermal dispersion (which are considered as 'true' values), and $\Delta T_{o(i)}$ corresponds to the results from the analytical

Table 2Dispersivity range scenarios. Scenario 1: thermal dispersion is assumed to be only dependent on the Darcy velocity (REV: Representative elementary volume). Scenario 2: thermal dispersion is assumed to be scale-dependent.

Scenario	Dispersivity	Field scale
1	$\alpha_x = 1 \times 10^{-2} \text{ m}$	REV
	$\alpha_y = 3.3 \times 10^{-3} \text{ m}$	
2	$\alpha_{x} = 0.5 - 2.0 \text{ m}$	10 m
	$\alpha_y = 0.05 - 0.2 \text{ m}$	

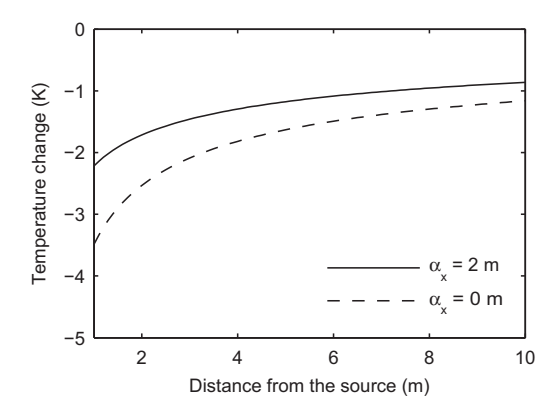


Fig. 3. Temperature profiles along the centerline for steady state conditions with and without thermal dispersion ($q=2\times 10^{-6}$ m/s, y=0 m). RMSE = 0.56 K (eq. (21)).

solution with only diffusion ($\lambda_d = 0$). As an empirical threshold, we consider that RMSE values <0.1 K represent conditions in which the influence of thermal dispersion is marginal enough to be ignored. This is based on the typical measurement accuracy of temperature.

5. Results and discussion

5.1. Effect of thermal dispersion on the temperature response

Discrepancies of the temperature response distribution for steady state conditions are depicted by contour maps of root mean square error (RMSE) for a bulk thermal conductivity of the porous medium of 2.5 W/m/K (Fig. 4a) and 4.0 W/m/K (Fig. 4b). The contours delineate the RMSE of the temperature change with and without thermal dispersivity for a distance of 1 m-10 m downgradient from the source in dependence on Darcy flow velocity. As expected, the larger the neglected thermal dispersivity, the larger the RMSE of the calculated temperature distribution. What is more, the error also increases with rising Darcy velocities (Fig. 4). This reflects the effect of the thermal dispersion on the temperature plume distribution in steady state conditions. It has to be mentioned, however, that for high dispersivity and Darcy velocity scenarios ($\alpha_x > 1$ m; $q > 5 \times 10^{-6}$ m/s), the RMSE slightly decreases. Under these conditions, the temperature profile becomes quite flat due to the dissipated energy and therefore the RMSE decreases.

Ignoring longitudinal dispersivities of less than 0.1 m yields RMSE values lower than 0.1 K. Therefore, for the range of flow velocities taken in this study, the influence of thermal dispersion given by scenario 1 ($\alpha_x = 1 \times 10^{-2}$ m) is marginal enough to be ignored. In this sense, if we assume that macroscopic heterogeneities of the hydraulic conductivity field do not have an effect on the thermal dispersion (i.e., homogeneous aquifer), then thermal dispersion given only by the dependence on the Darcy velocity has no major influence on the temperature plume distribution.

For the range of thermal dispersivities given by scenario 2 ($\alpha_x = 0.5-2$ m), the RMSE varies up to 0.56 K for $\lambda_0 = 2.5$ W/m/K depending on the Darcy velocity. For this specific case, only for Darcy velocities around 10^{-8} m/s the RMSE is less than 0.1 K for most of the dispersivity range. For larger velocities, the error can be higher than 0.1 K. For instance, if thermal dispersion if neglected for a longitudinal dispersivity of 2 m and a Darcy velocity of 1×10^{-6} m/s, the RMSE is about 0.56 K, which is about 23% of the maximum temperature change (2.4 K) in the temperature profile (Fig. 3). In order to evaluate the effect of the thermal conductivity when neglecting thermal dispersion, a higher value of λ_0 (4.0 W/m/K) is assumed (Fig. 4b). As we can see, an increase in thermal conductivity results in a lower effect of neglecting thermal

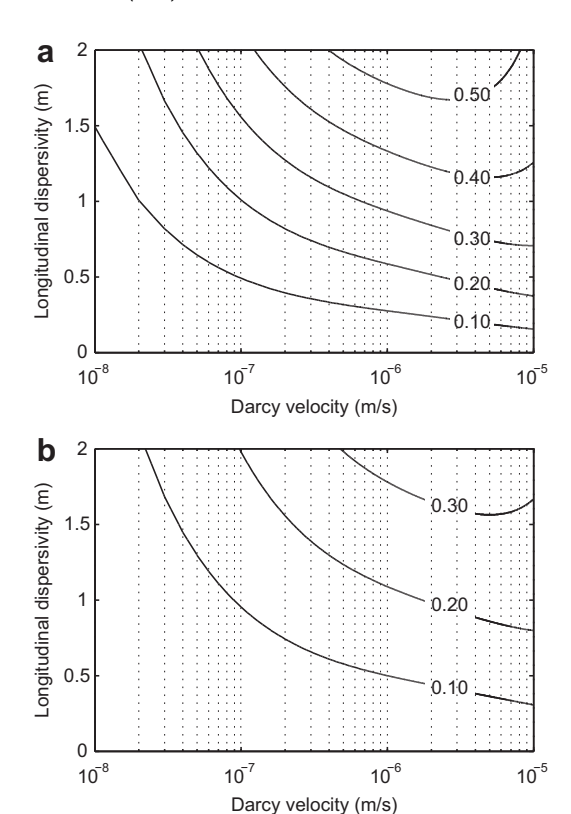


Fig. 4. Contour maps of RMSE [K] in dependence on Darcy velocity for steady state conditions with and without thermal dispersion (downgradient distance range x = 1-10 m): (a) $\lambda_0 = 2.5$ W/m/K, (b) $\lambda_0 = 4.0$ W/m/K.

dispersion. For instance, neglecting a thermal dispersivity of 1.5 m with a $q=1\times 10^{-8}$ m/s yields an RMSE =0.1 K for a thermal conductivity of 2.5 W/m in steady state conditions, whereas for a higher thermal conductivity of 4.0 W/m, the same Darcy velocity yields an RMSE <<0.1 K.

For transient conditions, the discrepancies of the temperature plume distribution are shown in Fig. 5 for different aquifer materials. Fine sand, medium sand, coarse sand and gravel aquifers are evaluated with a Darcy velocity of 10^{-8} m/s, 10^{-7} m/s, 10^{-6} m/s and 10^{-5} m/s, respectively. Moreover, the selected simulation times are based on the instant when longitudinal dispersion is more dominant over the transverse one at a distance of 10 m for each Darcy

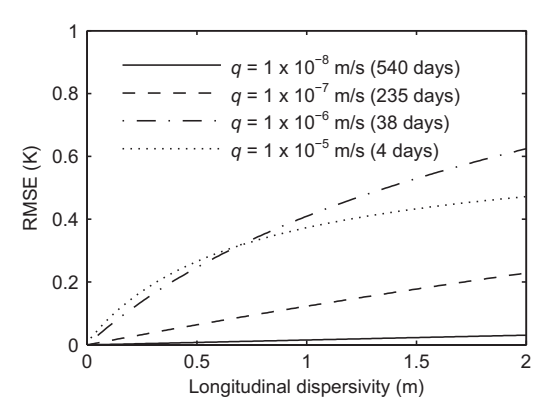


Fig. 5. RMSE as a function of Darcy velocity for transient conditions with and without thermal dispersion. Fine sand, medium sand, coarse sand and gravel aquifers are simulated with a Darcy velocity of 10^{-8} m/s, 10^{-7} m/s, 10^{-6} m/s and 10^{-5} m/s, respectively (x = 0.1–10 m, $\lambda_0 = 2.5$ W/m/K).

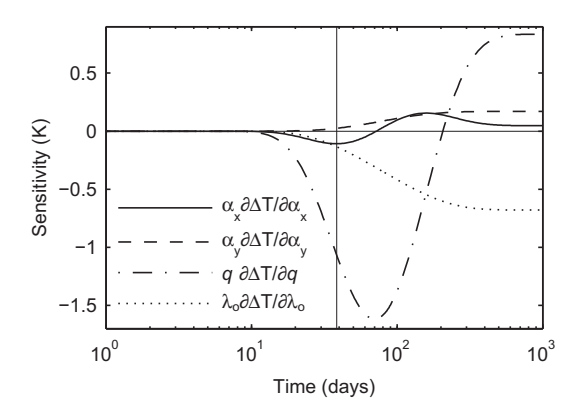


Fig. 6. Relative sensitivities of equation (14) at a distance of 10 m downgradient from the source ($q = 1 \times 10^{-6}$ m/s). It shows the sensitivity of the temperature change (ΔT) to variations of the longitudinal dispersivity α_{x_0} transverse dispersivity α_{y_0} bulk thermal conductivity of porous medium λ_{v_0} , and Darcy velocity q as a function of time.

velocity (Fig. 6). Similar to steady state conditions, under transient conditions the influence of thermal dispersion based on scenario 1 is minor. For scenario 2, it can be seen that the RMSE varies up to 0.6 K. Only for Darcy velocities of 10^{-8} m/s is the RMSE less than 0.1 K for the whole range of neglected longitudinal dispersivity. For Darcy velocities of 10^{-7} m/s, the RMSE only exceeds 0.1 K for longitudinal dispersivities larger than 0.8 m. On the other hand, for coarse sand and gravel aquifers (10^{-6} m/s, 10^{-5} m/s) the RMSE increases up to 0.6 K. These results, however, might vary depending on the examined transient times.

5.2. Development of the temperature plume length

The analytical equation for steady state conditions (eq. (13)) is computed in two dimensions. Fig. 7 depicts relative temperature contours (isotherms) for different values of thermal dispersivity. Relative temperature means that the isotherms delineate a temperature difference of $\Delta T = -1$ K between plume and ambient conditions. It can be observed that the temperature plume gets shorter with increasing dispersivity. This is attributed to the fact that for steady state conditions, longitudinal dispersivity is not as important as the transverse one. For long time simulation, the relative sensitivity of longitudinal dispersivity almost disappears while transverse dispersivity reaches its maximum in equation (12) (Fig. 6). Hence, spreading of heat in the transverse direction to flow causes dissipation of energy. Apparently, a dispersion-dominated regime yields lower temperature changes close to the source, i.e.,

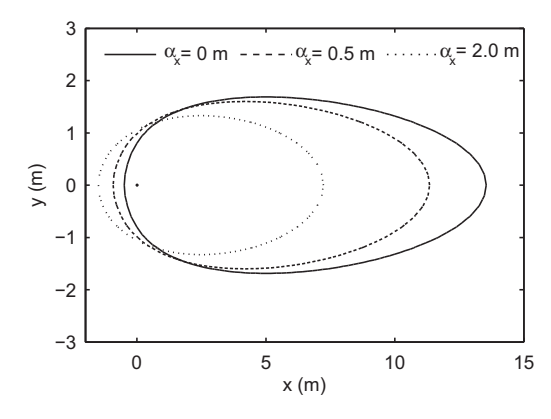


Fig. 7. Temperature plumes in steady state conditions for different thermal dispersivities in a coarse sand aquifer ($\Delta T = -1$ K, $q = 2.0 \times 10^{-6}$ m/s).

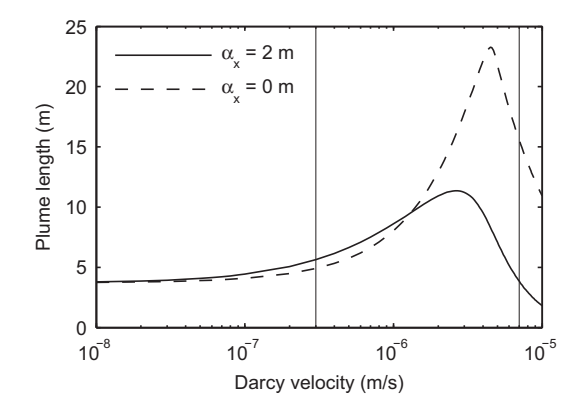


Fig. 8. Plume length as a function of the Darcy velocity ($\lambda_0 = 2.5 \text{ W/m/K}$, $q_L = -60 \text{ W/m}$, t = 50 days, $\Delta T = -0.5 \text{ K}$).

the BHE, in steady state conditions in comparison to scenarios without thermal dispersion. Therefore, neglecting thermal dispersion results in an overestimation of the temperature plume length under steady state conditions.

For transient conditions some temperature isotherms can reach greater distances when increasing thermal dispersion. Fig. 8, for instance, shows that neglecting a thermal dispersivity of 2 m with a Darcy velocity of 3×10^{-7} m/s results in an underestimation of the temperature plume length of around 1 m. This is due to the dominance of longitudinal dispersion over the transverse dispersion at this specific point for transient conditions.

Fig. 8 shows the behavior of the temperature plume length as a function of Darcy velocity. For the specific case shown in this figure (t=50 days, $\Delta T=-0.5$ K), we can see that the temperature plume length first increases over a range of velocities in which there are still transient conditions and the longitudinal dispersion prevails over the transverse one. Then, there is a transition between transient and steady state conditions and finally the temperature plume decreases as higher values of Darcy velocity are assumed.

For a Darcy velocity of 7.0×10^{-6} m/s, the heat plume for a temperature change of -0.5 K is 4 m long considering a longitudinal dispersivity of 2 m. Ignoring the thermal dispersivity, the calculated plume length is 15 m. Such a discrepancy can be critical for licensing GSHP systems, e.g., if the suggested distance between neighboring boreholes is 10 m.

6. Conclusions

An analytical modeling study of the effect of neglecting thermal dispersion under different groundwater flow and dispersion conditions is carried out. For this purpose, analytical solutions to simulate heat transport in the subsurface for steady state and transient conditions are applied. Moreover, an equation to calculate the length of the temperature plume for steady state is developed. Our criterion for assessing the influence of thermal dispersion on the temperature plumes created by the use of GSHP systems is the calculated error that would be introduced. Therefore, the root mean square error (RMSE) is taken to quantify the discrepancy between results with and without thermal dispersion. The RMSE rises with increasing values of the ignored thermal dispersivity. What is more, it also increases with larger Darcy velocities.

It has to be mentioned that a fixed hydraulic gradient of 10^{-3} was assumed. Therefore, the results are based on this assumption. For homogenous aquifers in which the thermal dispersion depends only on the magnitude of groundwater flow, the effect of thermal dispersion on the temperature plume distribution around the BHE is minor (RMSE << 0.1 K) under steady state and transient

conditions. On the other hand, if thermal dispersion is assumed to be scale-dependent and if the development of the temperature profiles and the extension of the temperature plumes are of concern, neglecting thermal dispersion is critical for conditions typical for medium sand to gravel aquifers (with Darcy velocities $q>10^{-8}\,$ m/s) for steady state and transient conditions. For geological conditions dominated by fine sand ($q=10^{-8}\,$ m/s), the assumption of neglecting thermal dispersion must be carefully evaluated depending on the case-specific thermal conductivity and thermal dispersivity. An increase in thermal conductivity results in a lesser effect of ignoring thermal dispersion.

Thermal dispersion causes dissipation of energy. Temperature plume lengths become shorter with increasing thermal dispersion for steady state conditions. Apparently, a dispersion-dominated regime yields lower temperature changes close to the source, i.e., the BHE, in comparison to scenarios without thermal dispersion. For transient conditions, however, temperature plume lengths for certain isotherms can become larger with increasing thermal dispersion.

We can conclude that the consideration of the thermal dispersion is an important factor regarding the temperature plumes in the subsurface that develop from GSHP systems for sand and gravel aquifers. From the perspective of environmental regulators, such assumptions might be crucial for licensing applications and sustainable operation of neighboring GSHP systems. In comparison, ignoring thermal dispersion provides appropriate predictions of the extension and shape of temperature plumes for flow conditions typical for geological formations dominated by fine sands, clays, and silts with $q<10^{-8}$ m/s. Accordingly, the range of hydrogeological conditions in which the thermal dispersivity can be ignored is still large. This might be the reason why thermal dispersion has been traditionally neglected in heat transport simulation problems.

It has to be mentioned here that the presented results are based on the selected RMSE (root mean square error) threshold (RMSE > 0.1 K). In addition, it should be kept in mind that errors related to the determination of hydraulic conductivity [55] might lead to higher uncertainty in the determination of temperature plumes than those related to neglecting thermal dispersion.

Finally, the range of dispersivity values chosen in this study is based on a field scale of 10 m. For larger distances and assuming scale-dependency, thermal dispersivities can be higher and consequently have greater influence on the extension of the simulated temperatures plumes and induced temperature changes.

Acknowledgements

The financial support from the International Postgraduate Studies in Water Technologies (IPSWaT) by the Federal Ministry for Education and Research (BMBF) of Germany for the first author is profoundly acknowledged. The work was also supported by the EU 7th framework program (ECO-GHP project). The support of Margaret Hass in preparing the manuscript is also gratefully acknowledged. Finally, we thank the four anonymous reviewers for their helpful comments and suggestions that improved the quality of the manuscript.

References

- J.W. Lund, D.H. Freeston, T.L. Boyd, Direct application of geothermal energy: 2005 worldwide review, Geothermics 34 (6) (2005) 691–727.
- [2] B. Sanner, C. Karytsas, D. Mendrinos, L. Rybach, Current status of ground source heat pumps and underground thermal energy storage in Europe, Geothermics 32 (2003) 579–588.
- [3] A. Mustafa Omer, Ground-source heat pumps systems and applications, Renew. Sustain. Energ. Rev. 12 (2) (2008) 344–371.
- [4] P. Blum, G. Campillo, W. Münch, T. Kölbel, CO₂ savings of ground source heat pump systems – a regional analysis, Renew. Energ. 35 (1) (2010) 122–127.

- [5] D. Saner, R. Juraske, M. Kübert, P. Blum, S. Hellweg, P. Bayer, Is it only CO₂ that matters? A life cycle perspective on shallow geothermal systems, Renew. Sustain. Energ. Rev. 14 (7) (2010) 1798–1813.
- [6] J. Hecht-Méndez, N. Molina-Giraldo, P. Blum, P. Bayer, Evaluating MT3DMS for heat transport simulation of closed shallow geothermal systems, Ground Water 48 (5) (2010) 741–756.
- [7] S. Hähnlein, N. Molina-Giraldo, P. Blum, P. Bayer, P. Grathwohl, Ausbreitung von Kältefahnen im Grundwasser bei Erdwärmesonden. (Cold plumes in groundwater for ground source heat pump systems), Grundwasser 15 (2010) 123–133.
- [8] S. Pannike, M. Kölling, B. Panteleit, J. Reichling, V. Scheps, H.D. Schulz, Auswirkung hydrogeologischer Kenngrößen auf die Kältefahnen von Erdwärmesondenanlagen in Lockersedimenten, Grundwasser 11 (2006) 6–18.
- [9] S. Hähnlein, P. Bayer, P. Blum, International legal status of the use of shallow geothermal energy, Renew. Sustain. Energ. Rev. 14 (2010) 2611–2625.
- [10] A.D. Chiasson, S.J. Rees, J.D. Spitler, A preliminary assessment of the effects of ground water flow on closed-loop ground-source heat pump systems, ASH-RAE Trans. 106 (1) (2000) 380–393.
- [11] R. Fan, Y. Jiang, Y. Yao, Z. Ma, Theoretical study on the performance of an integrated ground-source heat pump system in a whole year, Energy 33 (11) (2008) 1671–1679.
- [12] J.J. Hidalgo, J. Carrera, M. Dentz, Steady state heat transport in 3D heterogeneous porous media, Adv. Water Resour. 32 (8) (2009) 1206–1212.
- [13] H.S. Carslaw, J.C. Jäger, Conduction of Heat in Solids, second ed. Oxford University Press. New York. 1959.
- [14] S. Signorelli, S. Bassetti, D. Pahud, T. Kohl, Numerical evaluation of thermal response tests, Geothermics 36 (2) (2007) 141–166.
- [15] J. Bear, Dynamics of Fluids in Porous Media. American Elsevier Publishing Company Inc, New York, 1972.
- [16] D.W. Green, R.H. Perry, R.E. Babcock, Longitudinal dispersion of thermal energy through porous media with a flowing fluid, AIChE J. 10 (5) (1964).
- [17] G. de Marsily, Quantitative Hydrogeology. Academic Press, San Diego, California, 1986.
- [18] G. Ferguson, Heterogeneity and thermal modeling of ground water, Ground Water 45 (4) (2007) 485–490.
- [19] J.P. Sauty, A.C. Gringarten, H. Fabris, D. Thiery, A. Menjoz, P.A. Landel, Sensible energy storage in aquifers 2. Field experiments and comparison with theoretical results, Water Resour. Res. 18 (1) (1982) 253—265.
- [20] M.G. Sutton, D.W. Nutter, R.J. Couvillion, A ground resistance for vertical bore heat exchangers with groundwater flow, J. Energ. Resour. Tech. 125 (3) (2003) 183–189.
- [21] N. Diao, Q. Li, Z. Fang, Heat transfer in ground heat exchangers with groundwater advection, Int. J. Therm. Sci. 43 (12) (2004) 1203–1211.
- [22] D.A. Nield, A. Bejan, Convection in Porous Media, third ed. Springer, New York, 2006.
- [23] T. Metzger, S. Didierjean, D. Maillet, Optimal experimental estimation of thermal dispersion coefficients in porous media, Int. J. Heat Mass Transf. 47 (14–16) (2004) 3341–3353.
- [24] C. Moyne, S. Didierjean, H.P. Amaral Souto, O.T. da Silveira, Thermal dispersion in porous media: one-equation model, Int. J. Heat Mass Transf. 43 (20) (2000) 3853–3867.
- [25] H. Fujii, R. Itoi, J. Fujii, Y. Uchida, Optimizing the design of large-scale ground-coupled heat pump systems using groundwater and heat transport modeling, Geothermics 34 (3) (2005) 347–364.
- [26] A.D. Woodbury, L. Smith, On the thermal effects of three-dimensional groundwater flow, J. Geophys. Res. 90 (B1) (1985) 759–767.
- [27] P.A. Domenico, F.W. Schwartz, Physical and Chemical Hydrogeology, second ed. John Wiley & Sons Inc, New York, 1998.
- [28] C.T. Hsu, P. Cheng, Thermal dispersion in a porous medium, Int. J. Heat Mass Transf. 33 (8) (1990) 1587–1597.
- [29] X. Lu, Experimental investigation of thermal dispersion in saturated soils with one-dimensional water flow, Soil Sci. Soc. Am. J. 73 (6) (2009) 1912–1920.
- [30] M.H.J. Pedras, M.J.S. de Lemos, Thermal dispersion in porous media as a function of the solid—fluid conductivity ratio, Int. J. Heat Mass Transf. 51 (21–22) (2008) 5359–5367.
- [31] J. Levec, R.G. Carbonell, Longitudinal and lateral thermal dispersion in packed beds. Part II. Comparison between theory and experiment, AIChE J. 31 (4) (1985) 591–602.
- [32] J.P. Sauty, A.C. Gringarten, A. Menjoz, P.A. Landel, Sensible energy storage in aquifers 1. Theoretical study, Water Resour. Res. 18 (1982).
- [33] L. Smith, D.S. Chapman, On the thermal effects of groundwater flow 1. Regional scale systems, J. Geophys. Res. 88 (B1) (1983) 593–608.
- [34] J.W. Hopmans, J. Šimunek, K.L. Bristow, Indirect estimation of soil thermal properties and water flux using heat pulse probe measurements: geometry and dispersion effects, Water Resour. Res. 38 (1) (2002) 1006.
- [35] J. Constantz, Heat as a tracer to determine streambed water exchanges, Water Resour. Res. 44 (2008) W00D10. doi:10.1029/2008WR006996.
- [36] J.W. Molson, E.O. Frind, C.D. Palmer, Thermal energy storage in an unconfined aquifer: 2. Model development, validation, and application, Water Resour. Res. 28 (10) (1992) 2857–2867.
- [37] L.W. Gelhar, C. Welty, K.R. Rehfeldt, A critical review of data on field-scale dispersion in aquifers, Water Resour. Res. 28 (7) (1992) 1955–1974.
- [38] G.W. Su, J. Jasperse, D. Seymour, J. Constantz, Estimation of hydraulic conductivity in an alluvial system using temperatures, Ground Water 42 (6) (2004) 890–901.

- [39] C. Beyer, S. Bauer, O. Kolditz, Uncertainty assessment of contaminant plume length estimates in heterogeneous aquifers, J. Contam. Hydrol. 87 (1–2) (2006) 73–95.
- [40] M. Xu, Y. Eckstein, Use of weighted least-squares method in evaluation of the relationship between dispersivity and field scale, Ground Water 33 (6) (1995) 905–908.
- [41] D. Schulze-Makuch, Longitudinal dispersivity data and implications for scaling behavior, Ground Water 43 (3) (2005) 443–456.
- [42] S.P. Neuman, Universal scaling of hydraulic conductivities and dispersivities in geologic media, Water Resour. Res. 26 (8) (1990) 1749–1758.
- [43] C.B. Andrews, M.P. Anderson, Thermal alteration of groundwater caused by seepage from a cooling lake, Water Resour. Res. 15 (3) (1979) 595–602.
- [44] J. Constantz, M.H. Cox, G.W. Su, Comparison of heat and bromide as ground water tracers near streams, Ground Water 41 (5) (2003) 647–656.
- [45] C.E. Hatch, A.T. Fisher, J.S. Revenaugh, J. Constantz, C. Ruehl, Quantifying surface water—groundwater interactions using time series analysis of streambed thermal records: method development, Water Resour. Res. 42 (10) (2006) W10410.
- [46] G. Windqvist, H. Hyden, Heat Transfer in Groundwater VBB Rep. 92203543. VBB. Stockholm. 1976.
- [47] Z.-G. Yuan, W.H. Somerton, K.S. Udell, Thermal dispersion in thick-walled tubes as a model of porous media, Int. J. Heat Mass Transf. 34 (11) (1991) 2715–2726.

- [48] A. Vandenbohede, A. Louwyck, L. Lebbe, Conservative solute versus heat transport in porous media during push—pull tests, Transport Porous Med. 76 (2) (2008) 265–287.
- [49] P. Eskilson, 1987. Thermal analysis of heat extraction boreholes. Ph.D. Thesis. University of Lund, Lund, Sweden.
- [50] S. Zubair, M. Chaudhry, Temperature solutions due to time-dependent moving-line-heat sources, Heat Mass Transf. 31 (3) (1996) 185–189.
- [51] M. Abramowitz, I.S. Stegun, Handbook of Mathematical Functions. With Formulas, Graphs and Mathematical Tables. Dover Publications Inc., New York, 1964.
- [52] VDI, Verein Deutscher Ingenieure, Blatt 1: Thermische Nutzung des Untergrundes-Grundlagen, Genehmigungen, Umweltaspekte. (Part 1: Thermal Use of the Underground-Fundamentals, Approvals, Environmental Aspects) (2000) VDI-4640/1.
- [53] K. Spitz, J. Moreno, A Practical Guide to Groundwater and Solute Transport Modeling. John Wiley & Sons Inc, New York, 1996.
- [54] VDI, Verein Deutscher Ingenieure, Blatt 2: Thermische Nutzung des Untergrundes-Erdgekoppelte Wärmepumpenanlagen. (Part 2: Thermal Use of the Underground-Ground Source Heat Pump Systems) (2001) VDI-4640/2.
- [55] S.C. Lessoff, U. Schneidewind, C. Leven, P. Blum, P. Dietrich, G. Dagan, Spatial characterization of the hydraulic conductivity using direct-push injection logging, Water Resour. Res. 46 (2010) W12502.